Epidemics 29 (2019) 100358

Contents lists available at ScienceDirect

Epidemics

journal homepage: www.elsevier.com/locate/epidemics

Analyzing influenza outbreaks in Russia using an age-structured dynamic transmission model

Vasiliy Leonenko[a,*], Georgiy Bobashev[b]

[a] ITMO University, Saint Petersburg, Russian Federation
[b] RTI International, Research Triangle Park, NC, USA

ARTICLE INFO

MSC:
37N25
65C20
92C60

Keywords:
Seasonal influenza
Background immunity
Mathematical modeling
Incidence data

ABSTRACT

In this study, we addressed the ability of a minimalistic SEIR model to satisfactorily describe influenza outbreak dynamics in Russian settings. For that purpose, we calibrated an age-specific influenza dynamics model to Russian acute respiratory infection (ARI) incidence data over 2009–2016 and assessed the variability of proportion of non-immune individuals in the population depending on the regarded city, the non-epidemic incidence baseline, the contact structure considered and the used calibration method. The experiments demonstrated the importance of distinguishing characteristics of different age groups, such as contact intensities and background immunity levels. It was also found that the current model calibration process, which relies mostly on ARI incidence, demonstrates notable variation of output parameter values. Employing additional sources of data, such as strain-specific influenza incidence and external assessments on underreporting levels in different age groups, might enhance the plausibility of parameter values obtained by model calibration, along with reducing the assessment variation.

1. Introduction

Outbreaks of influenza, one of the oldest and most widely spread human infectious diseases, result in 3 to 5 million cases of severe illness annually worldwide, and the mortality rate is from 250,000 to 500,000 individuals per year (WHO, 2014). Influenza also causes an increase in heart attacks and strokes (CDC, 2019) and other disease complications. To effectively restrain influenza epidemics and reduce mortality attributed to influenza complications, health care organsations analyze influenza dynamic predictions obtained with the help of statistical and mechanistic models (Ivannikov and Ismagulov, 1983; Cliff et al., 1986; Marinich et al., 2005). To produce accurate predictions, many factors should be taken into account, such as weather (He et al., 2013; Shaman et al., 2010; Yaari et al., 2013), variation of virus strains (Truscott et al., 2011), individual contact patterns, and background immunity levels (Konshina et al., 2017).

High-quality incidence data are critical for efficient model calibration; however, few surveillance systems have collected sufficiently long and high-quality time series. Researchers often have to rely on incomplete incidence data reported by hospitals, pneumonia and influenza mortality data, or social media data (Broniatowski et al., 2013). Thus, corresponding research into influenza spread is often dedicated to the following:

- Studies of pandemic flu outbreaks (e.g., 1918, 1956, 1968, bird flu and swine flu). In the case of pandemics, the immunity is often stated to be absent, whereas for seasonal influenza it is necessary to consider broadly unknown existing immunity of individuals in the population (Colizza et al., 2007; Cauchemez et al., 2008), which requires laboratory studies or at least long-term data for the previous years to derive the proportion of the immune individuals.
- Studies of a purely theoretical outbreak without fitting the model to data (Kumar et al., 2015).
- Studies of an influenza outbreak in some closed area, for instance, a university campus, hospital, or small neighborhood (Nichol et al., 2010). Attempts to perform a plausible simulation on a larger area often face issues concerning the availability of epidemiological and population data (Smieszek et al., 2011).
- Studies of sentinel surveilance systems (CDC reports) or indirect measures such as social media searches and reports (for example, “Flu Near You” (Flu Near You, 2019)).

A few influenza modeling studies, however, use long-term sentinel data - collected in Israel (Maccabi health maintenance organization, estimated 24% of nationwide coverage) (Yaari et al., 2013), England and Wales (Royal College of General Practitioners, coverage 1.7%) (Baguelin et al., 2013), Belgium (Sentinel General Practitioners network,

* Corresponding author.
E-mail address: vnleonenko@yandex.ru (V. Leonenko).

https://doi.org/10.1016/j.epidem.2019.100358
Received 7 September 2018; Received in revised form 18 July 2019; Accepted 19 July 2019
Available online 22 July 2019

nationwide coverage 1.8%) (Goeyvaerts et al., 2015), France ("Sentinelles" General Practitioners network, nationwide coverage 2%) (Cauchemez et al., 2008), Italy (INFLUNET General Practitioners network, nationwide coverage 2.3%), and the United States (ILINet, Outpatient Influenza-like Illness Surveillance Network, 2800 enrolled health care providers) (Yamana et al., 2017). One issue with such incidence data, in addition to limited coverage, is that they are available only as aggregates for large territories, i.e. in a form of country-level incidences, or, in the case of French and U.S. surveillance networks, incidences for the states/provinces comprising several urban territories and rural areas.

The situation with incidence data collection is different in Russia where for many years influenza has been a mandatory reportable disease. The availability of distinct long-term age-structured reports on influenza-like diseases for Russian metropolitan areas gives an opportunity to calibrate and validate models on high-quality data. In Saint Petersburg (formerly Leningrad) acute respiratory infection (ARI) incidence has been collected since 1935, which gives one of the longest known flu surveillance periods (Ivannikov and Ismagulov, 1983). In 1957, the all-USSR surveillance center was established, which eventually led to the possibility of predicting flu outbreaks in Soviet cities with fairly high accuracy (Cliff et al., 1986). At the moment the surveillance center, located in the Research Institute of Influenza in Saint Petersburg (Research Institute of Influenza website, 2019), collects weekly reports on cumulative ARI incidence in 49 Russian cities, which gives nationwide coverage of about 35% (WHO, 2019a).

With all named advantages of Russian acute respiratory infection long-term dataset, it also has some specifics which must be taken into account when one wants to use it for the model calibration:

- **Lack of separate registration of influenza-like illness (ILI) cases.** Since the symptoms of severe cases of ARI are very similar to those of influenza, and the laboratory analysis is required to tell one disease from another, in most of the healthcare surveillance systems, including the Russian one, the statistics on ARI and influenza incidence is calculated cumulatively. However, in Western European and US surveillance systems only influenza-like illness cases are taken into account (cases of acute respiratory infection with measured fever of more than 38 C and cough with onset within the past 10 days, according to definition of WHO (WHO (2019b))), whereas in Russian surveillance all ARI cases are taken into account. This fact poses a problem of separating influenza outbreak incidence data from seasonal ARI dynamics, especially if the former is preceeded by fluctuations of ARI caused by seasonal factors.
- **Under-reporting.** Russian ARI surveillance system, like most of such surveillance systems worldwide, collects incidence data based on the reporting of medically-attended ARI, thus it does not include asymptomatic cases and other infection cases which were not accompanied by a visit to healthcare facilities. The most represented group in terms of reporting are children aged 0-2. The older is the age group under consideration, the less cases of ARI are medically attended and thus reported. Reporting of ARI among the adults is strongly affected by various factors, e.g. their ability to take a paid leave at work, thus, the corresponding disease reporting coefficient is hard to be assessed. As a consequence, a disease dynamics model fitted to the incidence in one age group may demonstrate incidence for another age groups which dramatically contradicts the data.

In the current work, we perform simulation of influenza dynamics in Russian cities using age-structured ARI data for model calibration. To the authors' knowledge, the regarded dataset was not used for simulation purposes. The aim of the study was to assess the ability of minimalistic SEIR models to satisfactorily describe influenza dynamics in Russian settings and to provide assessment of background immunity levels in the population, depending on geographical areas and age groups. Specifically, due to the uncertainty in incidence data described above, our objective was to account for its influence in the model output.

2. Materials and methods

2.1. Transmission model

The age-structured model was derived from the Baroyan-Rvachev model (Baroyan et al., 1970; Leonenko et al., 2016b) by splitting the population into l age groups. It is represented by a system of difference equations, with the time step equal to one day. Following the notations introduced in (Ivannikov and Ismagulov, 1983), let x_t be a fraction of susceptibles in the population, y_t be a number of newly *infected* individuals at moment t and $\overline{y_t}$ – a cumulative number of *infectious* persons by time t. Let N be a total population size which is considered constant during the epidemic season. The proportion of population which is vulnerable to the currently circulating flu virus strain is denoted by $\alpha \in [0; 1]$, and the remaining population is considered immune to infection. Then, the system of equations may be written in the following manner:

$$\begin{aligned} \bar{y}_t^{(j)} &= \sum_{\tau=0}^{T} y_{t-\tau}^{(j)} g_\tau, \; j \in \overline{0, l}, \\ y_{t+1}^{(j)} &= \Sigma_i \frac{\beta_{i,j}}{N} x_t^{(j)} \bar{y}_t^{(i)}, \; i, j \in \overline{0, l} \end{aligned} \tag{1}$$

$$\begin{aligned} x_{t+1}^{(j)} &= x_t^{(j)} - y_{t+1}^{(j)}, \; j \in \overline{0, l} \\ x_0^{(j)} &= \alpha_j N_j, \; j \in \overline{0, l}. \end{aligned} \tag{2}$$

The piecewise constant function g_τ gives a proportion of infectious individuals in a group of individuals infected τ days before the current moment t. The function reflects the change of individual infectiousness over time from the moment of acquiring influenza. We assume that there exists some moment $\bar{t}$: $\forall\, t \geq \bar{t}\;\; g_\tau = 0$, which corresponds to the moment of recovery. The values of $g(\tau)$ were set according to (Baroyan et al., 1970): $g(0) = g(1) = 0$, $g(2) = 0.9$, $g(3) = 0.9$, $g(4) = 0.55$, $g(5) = 0.3$, $g(6) = 0.15$, $g(7) = 0.05$, $g(8) = g(9) = ...=0$.

Following the social contact hypothesis (Wallinga et al., 2006), we assume that $\beta_{ij} = \lambda \cdot \delta_{ij}$, where λ is the virulence of a current flu strain and δ_{ij} is the daily number of contacts with people from age group j reported by survey participants from age group i, where $i, j \in \overline{1, l}$. The values δ_{ij} constitute the contact matrix $C = C(i, j)$.

2.2. Data

2.2.1. Original data

The original dataset provided by Research Insititute of Influenza contains weekly ARI incidence in 49 Russian cities for four age groups (0–2, 3–6, 7–14, and 15+) in 1990–2016. In addition to incidence numbers, the dataset contains markers for weeks which correspond to the period of officially declared influenza epidemic. The weeks corresponding to an influenza outbreaks are assessed in the Research Institute of Influenza on the base of epidemic thesholds. A documented method based on the t-test is used to caclulate epidemic thresholds for each week relying on long-term average level for seasonal ARI (Marinich et al., 2005).

For the purpose of our study, we used ARI incidence for two urban areas: Omsk (about 1.2 million inhabitants) and Saint Petersburg (approximately 4.8 million). These cities are located in different climate zones and have different patterns of transport flow (both for intercity migration and urban commuting), which might affect disease dynamics. We took a subset of ARI incidence data for 2009–2016, which corresponds to the period of circulation of a pandemic A(H1N1)pdm09 flu virus strain (Konshina et al., 2017). A(H1N1)pdm09 was not the only strain circulating within Russia during those years; a number of infection cases were also caused by A(H3N2) (particularly in the 2011–2012 and 2014–2015 seasons) and B strains (for more details on circulating strains see (Konshina et al., 2017)). Due to lack of strain-specific incidence data, and following the ideas of another modeling studies, for instance, (Goeyvaerts et al., 2015), in our model we consider that the

regarded series of epidemic processes are caused by circulation of one generic virus strain.

2.2.2. Day to week conversion

In the model, we consider the time step equal to one day; on the other hand, ARI incidence data are collected on a weekly basis. Whereas in the earlier studies (Leonenko et al., 2016a) we converted weekly incidence data to a daily one using cubic interpolation, in the current paper we sum daily incidences calculated by the model to derive weekly data to match them with the original ARI incidence.

2.2.3. Epidemic curves extraction

As it was mentioned in the "Introduction" section, one of the tasks one needs to accomplish when working with Russian ARI dataset is to extract epidemic incidence from seasonal ARI data. The officially stated epidemic periods are calculated implying rather high epidemic thresholds and thus might include only a part the outbreak curve and omit some of the minor outbreaks. In our method of epidemic curve extraction, we consider the existence of a long-term baseline ARI level which makes it possible to distinguish epidemic outbreaks from seasonal ARI incidence. Since we regard incidence data for several years, we postulate that the average ARI level does not depend on time and can be defined by some constant value a. We also assume that all the ARI cases exceeding the baseline are attributed to influenza, although ARI incidence is known to grow during influenza outbreaks and contribute to the epidemic incidence (Romanyukha et al., 2011). For each of the consequential ARI seasons (corresponding to a time period from week 26 of a fixed year to week 25 of the following year) we derive a single influenza epidemic incidence dataset.

2.3. Model calibration procedure

2.3.1. Optimization criterion

Let $Z_i^{(dat)}$ be a set of incidence data points corresponding to one particular outbreak in one regarded age group i, $i \in \overline{1,4}$. Let t_i be duration of the outbreak in an age group i in weeks and, correspondingly, the number of incidence values available for model fitting. The optimum criterion is defined as a squared difference between the incidence values taken from data and the values calculated by the model:

$$F(Z_1^{(dat)}, \ldots Z_4^{(dat)}, Z_1^{(mod)}, \ldots Z_4^{(dat)}) = \sum_{i=1}^{4} \Sigma_{k=0}^{t_i} w_{k,i} (z_i^{(mod)}(k) - z_i^{(dat)}(k))^2 \to min. \tag{3}$$

Here $z_i^{(dat)}(k)$ and $z_i^{(mod)}(k)$ are relative incidences on the k-th *week* taken from the input dataset and derived from the model correspondingly. Weights $w_{k,i}$ could be all set equal to 1 or changed to reflect the varied impact of assessment quality for different incidence points, their role will be described in detail in the "Simulation" section.

To match model time steps with actual weeks from the ARI incidence dataset, we need to align the timelines, either by an outbreak starting week (week 0 of the model is set to be equal to the first incidence value in the regarded dataset) or by the week of a maximal disease incidence (the week of the incidence peak in the model is considered equal to the week of the incidence peak in the dataset). Both methods have their advantages and disadvantages, their comparison for Russian ARI data was described by the authors in (Leonenko and Ivanov, 2018). In the current study, we used the alignment by peaks. Since we regard four age groups and their disease peaks might not coincide in time, we consequently choose a week of a model peak of each of the four groups as an alignment point, obtain four values of optimal parameter sets and finally select the best fit. In another words:

- For each age group i, $i \in \overline{1,4}$, (0–2, 3–6, 7–14, or 15+ years):
  - Assume that the model incidence curve for i-th age group has the maximum in the same week that the incidence data curve.
  - Using the optimization procedure, find the best fit $F_i^{(opt)}$.
- The index j, which corresponds to the age group selected for peak alighment, is selected to match minimal $F_i^{(opt)}$, i.e. $F_j^{(opt)} \le F_i^{(opt)} \ \forall \ i \in \overline{1,4}$.

To characterise the obtained quality of fit, we use coefficient of determination $R^2 \le 1$ which is calculated from the value of $F_j^{(opt)}$ and shows the percentage of the response variable variation that is explained by a model.

2.3.2. Calibration algorithm

To perform the optimization and to assess the model parameters, we used the computational algorithms implemented as a collection of scripts in Python programming language (Python 3.x with numpy and matplotlib libraries was used). The procedure scipy.optimize.minimize (Seleznev and Leonenko, 2017) with limited-memory BFGS optimization method (Liu and Nocedal, 1989) was employed. The issue which may affect the result of the optimization procedure according to criterion (3) is a possible convergence of the algorithm to local minima, caused by erroneous choice of initial values; hence, the parameter values that are found by the algorithm might not be optimal (Leonenko and Ivanov, 2018). To avoid this outcome, we incorporated simulated annealing optimization (Kirkpatrick et al., 1983) into our algorithm. Simulated annealing perturbs parameters to avoid convergence to a local minima, and finds the values of the optimized parameters that are close to the global minimum. Those values are subsequently used as the initial values in the BFGS method. The scheme of the resulting algorithm is demonstrated in Fig. 1.

3. Simulations

3.1. Simulation parameters

3.1.1. Model parameters

The aim of the simulations was to assess variability of parameter values and errors in epidemic peak heights demonstrated by the model, depending on the age group, regarded city, the choice of ARI baseline and the contact structure of the population.

The parameter values used for the simulations are listed in Table 1. Since we did not have any *a priori* knowledge to obtain preliminary assessments of the ranges of model variables α_i and λ, we took rather wide ranges for them, regarding two different ones (standard and extended) to see whether the selection of intervals influence the final assessments of these parameters. The experiments demonstrated that the upper bound for parameter values is rarely reached and in case of its extension the subsequent changes of the resulting calibrated parameter values are slight (see Appendix E).

3.1.2. Contact matrix

Defining effective contacts in the model (contacts which lead to infection transmision), we followed a methodology introduced in the POLYMOD study for Europe (Mossong et al., 2008), where "contact" is a two-way conversation of at least five words in the physical presence of another person. To estimate a contact matrix for our study, we used age-structured data from (Ajelli and Litvinova, 2017) which contains assessments of the daily number of contacts between groups of ages 0–4, 5–9, 10–15, …, 55+ for Tomsk, Russia (see Fig. 2). The details of the matrix recalculation algorithm are described in Appendix A, the resulting matrix used in the simulations is

$$C = \begin{pmatrix} 0.14 & 0.42 & 0.51 & 3.61 \\ 0.3 & 2.56 & 3.77 & 4.89 \\ 0.33 & 2.46 & 11.88 & 8.02 \\ 0.06 & 0.12 & 0.38 & 4.66 \end{pmatrix} \tag{4}$$

In one set of simulations, we used the contact matrix (4) (corresponds to heterogeneous mixing of the population). In another one, we assumed that the number of contacts for any two given age groups is the same and equal to the average contact number in the population

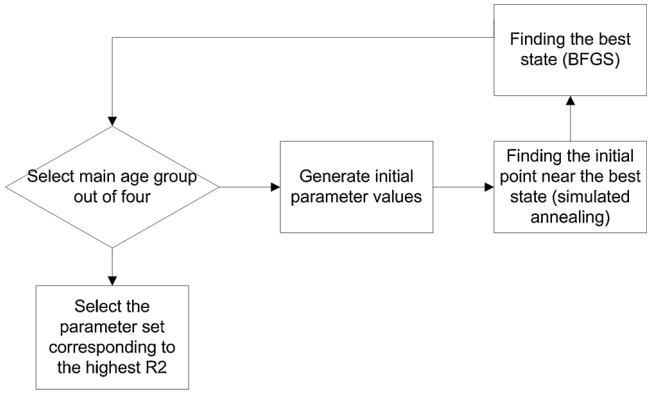

Fig. 1. A scheme of the calibration algorithm.

(corresponds to homogeneous mixing). Based on data from (3), the average contact intensity was set to 6.528.

3.1.3. Baseline variation

To assess the impact of baseline selection on the model calibration, we performed simulations with a number of different values of a, the long-term ARI baseline level. As an initial guess, for each age group we set a equal to average ARI incidence in that group during the regarded time period. For testing, we formed a baseline range by multiplying the average ARI incidence by a set of constants from 0.5 to 1.5 (+/-50%) with a step equal to 0.1. Thus, the tested incidence levels were within the interval *[0.5a, 1.5a]* (a blue stripe in Fig. 3). In addition to the mentioned range of ARI levels, we regarded a standard ARI baseline level for Research Institute of Influenza. This level is calculated as an average incidence of non-epidemic ARI during an epidemic season (week 40 of the regarded year to week 20 of the next year, corresponds to time from early autumn to late spring). Depending on city, year and age group, non-epidemic ARI level corresponds to *1.08a…1.2a* (see Table 2).

3.1.4. Procedure for forming the calibration dataset

As it can be seen from Fig. 3 (red lines), not all the points that visually belong to the epidemic wave are marked as epidemic incidence points. Morover, in some age groups an influenza outbreak might not exceed the epidemic threshold because of low corresponding incidence (for instance, it was commonplace for A(H3N2) epidemic in 2011–2012). To be able to perform model calibration to data with few marked points, we implemented adding incidence points before and after the marked ones to the calibration data. Therefore, the epidemic incidence dataset is formed in the following way:

- For the current season, city, and age group, the dataset includes all the incidence values with epidemic marks, plus Δ incidence values before and after the officially declared epidemic (by default, Δ= 1).
- If there was no officially declared epidemic during the regarded season, the dataset includes incidence values corresponding to time moments $t_p - \Delta$, $t_p - (\Delta - 1)$, ⋯, t_p, ⋯, $t_p + \Delta$, where t_p is the moment of ARI incidence peak (the maximum value).
- From each value of the dataset we subtract the assessed baseline ARI level y, thus obtaining the influenza incidence values.

Table 1
Model parameters.

Definition	Description	Values
α_i	Proportion of susceptible individuals in the population	Standard range: [0.001; 0.8] Extended range: [0.001; 1.0]
λ	Virulence of current flu strain	Standard range: [0. 001; 10.0] Extended range: [0.001; 12.0]
δ_{ij}	Daily number of contacts between the age groups i and j	Fixed (see below)

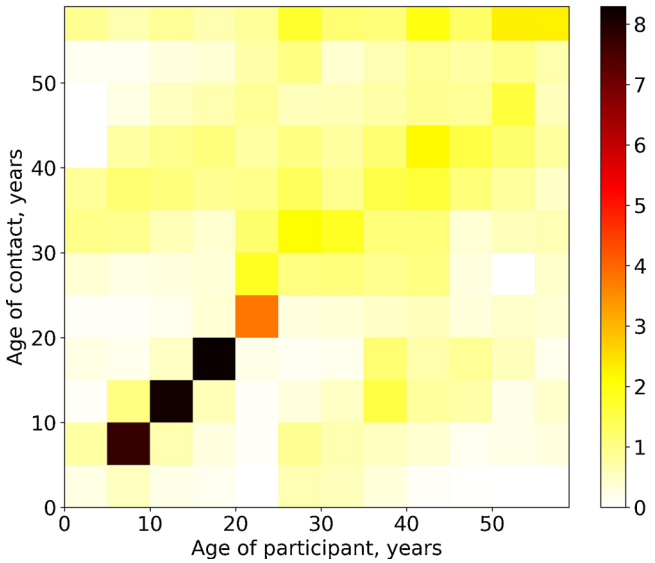

Fig. 2. Age-specific daily contact rates obtained for Tomsk, Russia (Ajelli and Litvinova, 2017).

An example of the calibration data for the baseline ARI level $y = a$ (average long-term all-year ARI incidence) is presented in Fig. 4.

For comparison purposes, we also prepared calibration data with Δ>1. Resulting from several launches of the calibration algorithm with various Δ, Δ= 5 was chosen. To compensate for addition of Δ non-epidemic points, which in some cases might not reflect the real outbreak incidence, and enhance the importance of data points which are closer to the incidence peak, we employed non-constant weights $w_{k,i}$ in the optimization formula (4). The corresponding formula that we used for weight calculation is $w_{k,i}(d) = \sigma^{-d}$, where d is the distance of the current data point from the peak in time units (weeks), $\sigma > 1$ regulates the rate of decreasing the "importance" of incidence points for the fitting procedure. In the same fashion, as it was made for the selection of Δ, we ran several preliminary simulations and ultimately have chosen $\sigma = 1.3$ as a value which gives an "optimal" decrease of $w_{k,i}$ over the distance to incidence peak. The type of calibration procedure with Δ= 5 and $\sigma = 1.3$ is later referred to as "enhanced calibration", opposed to a "standard" one with Δ= 1 and $\sigma = 1$ (in the latter case, all incidence points are equal in importance).

3.2. Simulation results

3.2.1. Influence of baseline selection and calibration method on calibration quality

The first series of simulations was performed to assess the role of baseline selection on model fit to incidence data and, consequently, to find the most plausible values of ARI threshold that separates influenza outbreak incidence from seasonal ARI. For that purpose, we used several indicators.

In Fig. 5, we demonstrate the distribution of ARI baseline level multipliers which corresponded to model curves with the highest coefficient of determination R^2. As it might be seen, the best fit is achieved for baseline levels within *[a, 1.5a]* for both calibration methods.

Another indicator used to assess the best ARI baseline level was the number of incidence curves for four age groups that was fitted to corresponding outbreak data with satisfactory accuracy. By "satisfactory

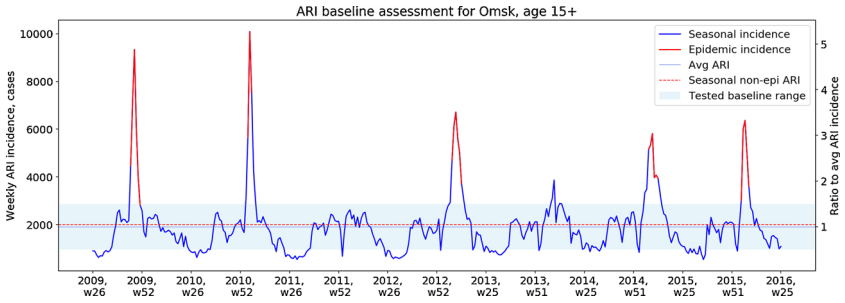

Fig. 3. Assessment of baseline ARI incidence level for Omsk, age group 15+.

Table 2
Correspondence of seasonal non-epidemic ARI levels to all-year ARI levels.

Age group, city	St. Petersburg	Omsk
0–2	1.2	1.09
3–6	1.18	1.11
7–14	1.17	1.11
15+	1.08	1.05

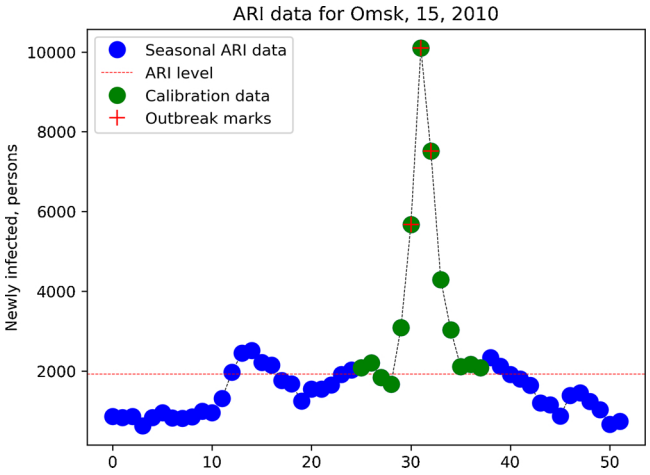

Fig. 4. Incidence values for model calibration, Omsk, age group 15+, epidemic season of 2010-2011. Blue dots correspond to ARI incidence data for a season under study, red crosses are marks of epidemic outbreaks registered by Research Institute of Influenza, green dots mark the choice of input for the calibration algorithm. (For interpretation of the references to colour in this figure legend, the reader is referred to the web version of this article).

accuracy" we imply the positive value of coefficient of determination, i.e. $R^2 > 0$, which means that the fitted curve describes the sample better than the mean of this sample. In the ideal case, the number of fitted curves should be 4, which corresponds to all regarded age groups. It might be seen from Fig. 6 that the average number of fitted curves in one outbreak grows with the growth of the multiplier, i.e. the fit quality increases. The biggest number of fitted curves is achieved for the baseline multipliers bigger than 1.0. Since the non-epidemic seasonal ARI baseline level has multipier values bigger than 1.0 (see Table 2), this level also demonstrates high number of fitted curves (see dashed horizontal lines in Fig. 6). Also, enhanced calibration (Fig. 6, lower) demonstrates better calibration results (more fitted curves in average) than the standard calibration (Fig. 6, upper). This result is justified by the dynamics of absolute error in peak height between the model and the data (Fig. 7), with the exception of the multiplier value equal to 1.3.

The results demonstrated in Figs. 5–7 might be interpreted in the following way. The ARI baseline level, which is optimal in terms of best model fitting, should correspond to or slightly exceed the all-year average ARI incidence. (It is worth noting that using the multiplier values bigger than 1.3..1.4 will place an ARI baseline higher than marked epidemic incidence (see Appendix B) which is not plausible.) Also, the employment of the enhanced calibration algorithm ($\Delta = 5$, $\sigma = 1.3$) results in better model fitting compared to a standard one.

Since it is showed that an average non-epidemic ARI incidence from week 40 to week 20, which is used as a baseline level in Research Institute of Influenza, corresponds to the multiplier values close to optimal, this incidence level will be used as a default baseline in the latter experiments, if not stated otherwise.

3.2.2. Calibration quality and proportion of susceptibles for different mixing assumptions

The second series of simulations were conducted to investigate the role of contact structure on the quality of model fit to data and the values of assessed model variables. We compared the homogeneous contact case (the contact intensities of individuals does not depend on their age groups) and heterogeneous case (contact matrix (4) is used). The corresponding fitted model curves are presented in Appendix C.

As it is shown in Fig. 8, the order of peak estimation error is merely influenced by variation of geographical location (Saint Petersburg and Omsk) and the chosen mixing assumption (homogeneous or heterogeneous). We can conclude that absence of a priori constraints on parameter values, along with scarcity of data (since the interval assessment is based on a sample of 14 points), may result in variability of the model output and thus put into doubt the necessity of accurate assessment of contact rates. This conclusion is consistent with the results presented in (Rahmandad and Sterman, 2008), where it was shown that variability in the model output because of parameter uncertainty may diminish the value of highly detailed models.

In both homogeneous and heterogeneous mixing cases, error values for the age group 15+ are predominantly positive (peak overestimation), whereas for the other groups they are mostly negative (peak underestimation). This effect might be explained by a number of factors including misspecification of the contact matrix and possible underreporting of flu incidence in the group of adults. Because adults often avoid visiting healthcare facilities when they have the flu, whereas children visit a physician more often in the same circumstances, the incidence registration of the latter could be considered more accurate. By calibrating the model solely to child incidence rates (i.e., excluding the incidence dynamics of age group 15+ from optimization criterion (3)) we may assess the prospected real incidence for adults – see Appendix D.

The assessments for α, the initial proportion of susceptibles, are demonstrated in Fig. 9. One can see that in case of homogeneous mixing for age group 0–2, the majority of values of α is shifted toward lower values (0.1 to 0.25), which does not seem plausible because it contradicts the generally weak flu immunity observed in small children compared to adults (Karpova et al., 2014). In case of heterogeneous mixing, the average value of α for individuals up to 2 years old are higher than those for other age groups, which seems closer to the data

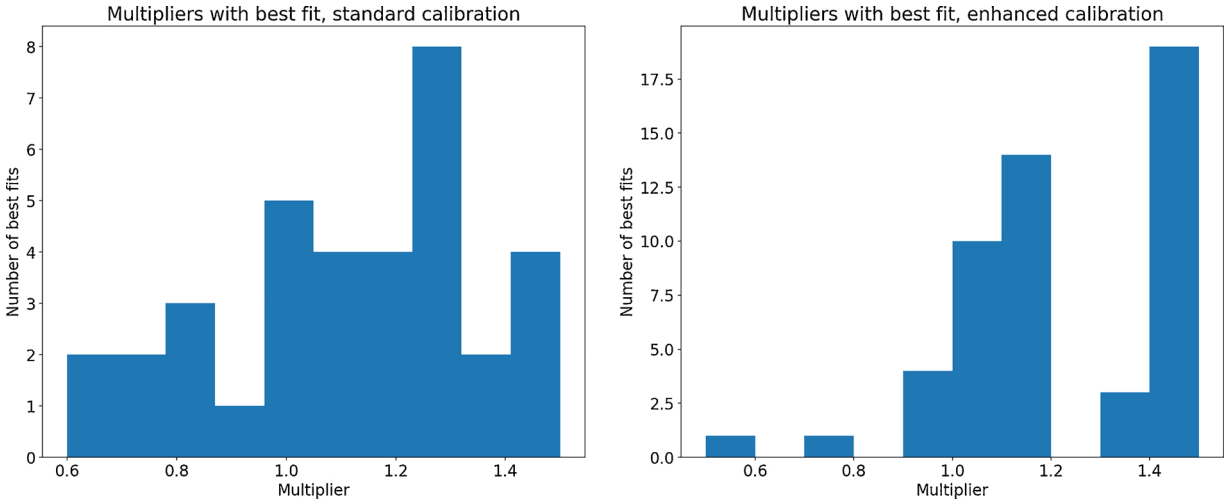

Fig. 5. Distribution of the multipliers corresponding to the best fitted curves for the selected city, year and age group.

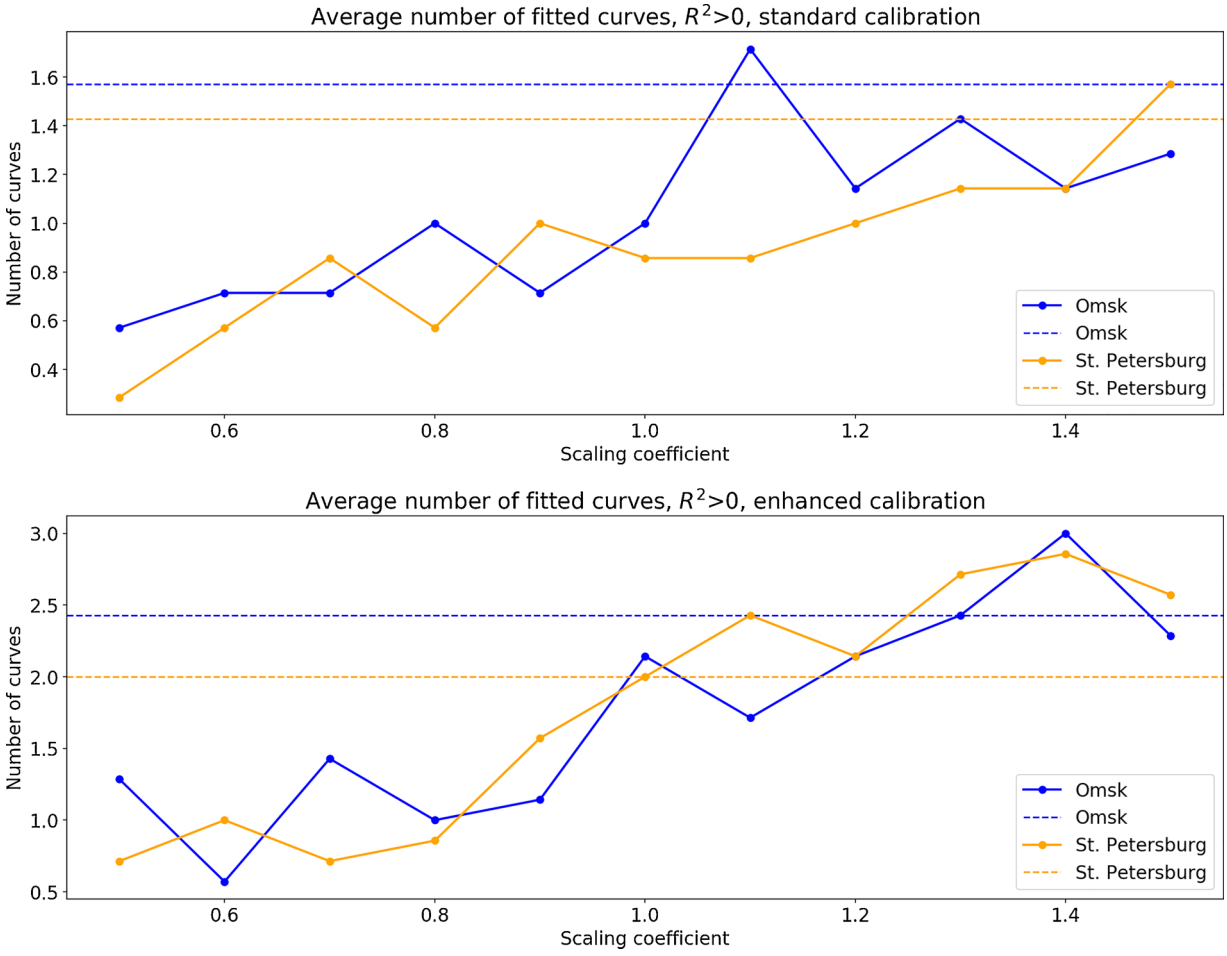

Fig. 6. Average number of fitted curves for 4 age groups in one outbreak calibration. Dashed lines correspond to the value for a non-epidemic ARI level.

obtained by laboratory studies.

The obtained results allow us to derive an assessment for $1-\alpha$, which corresponds to the proportion of population protected from infection. It is interesting to see that although the proportion of protected 15+ population is high in both cities, varying from 0.89 to 0.99, it does not prevent the epidemic in that age group. This situation might be explained by the fact that there is still a sufficient reservoir of susceptible adults in both cities, despite the high level of immunity, because of the big population in both citites (the resulting number of 15+ susceptibles has an order of magnitude around 10^4 for Omsk and 10^5 for Saint Petersburg). Also, it's clear that the infection is also brought to the 15+ group due to contacts with individuals from another age groups with lower immunity levels.

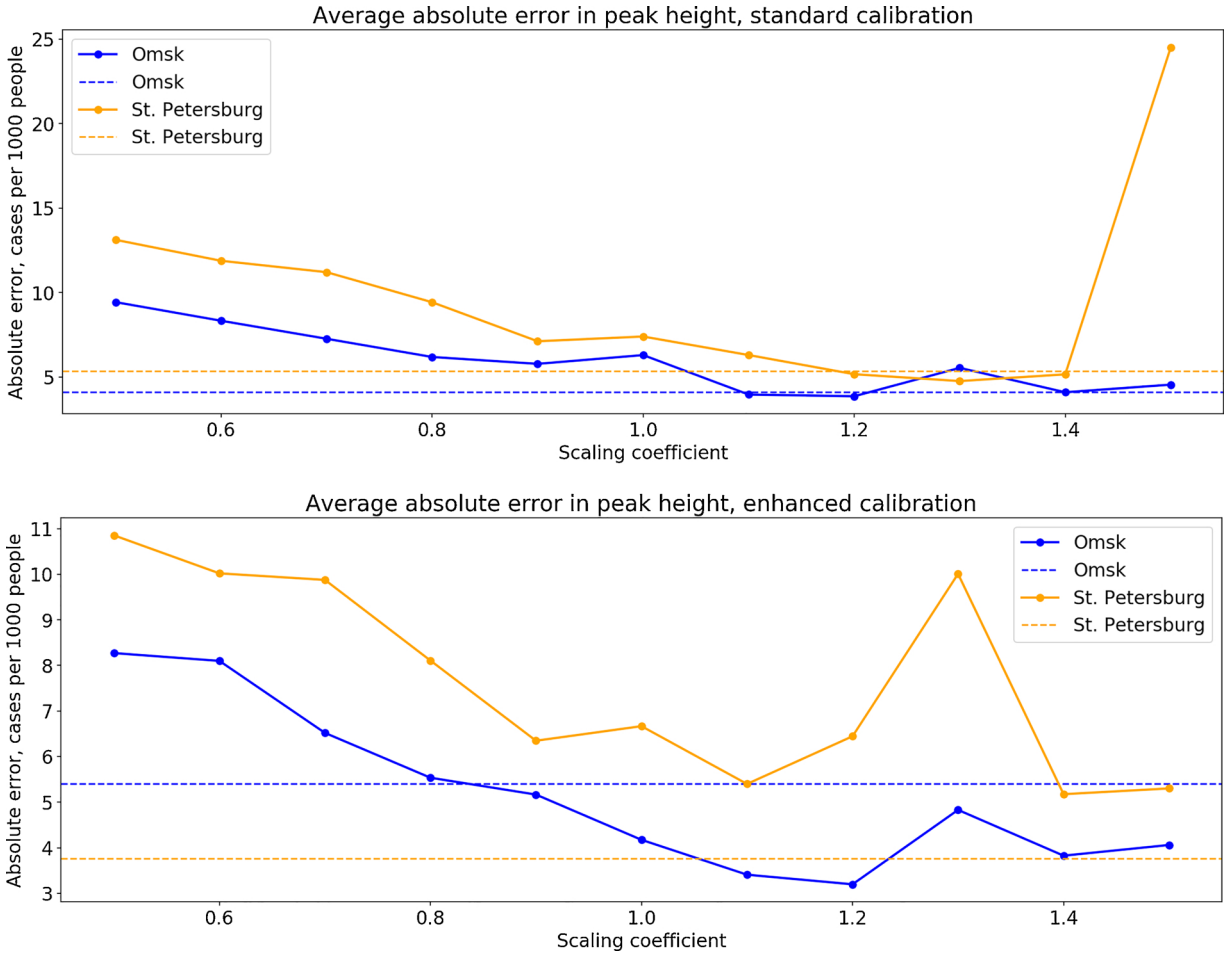

Fig. 7. Average absolute error in peak height between the model and the data. Dashed lines correspond to the value for a non-epidemic ARI level.

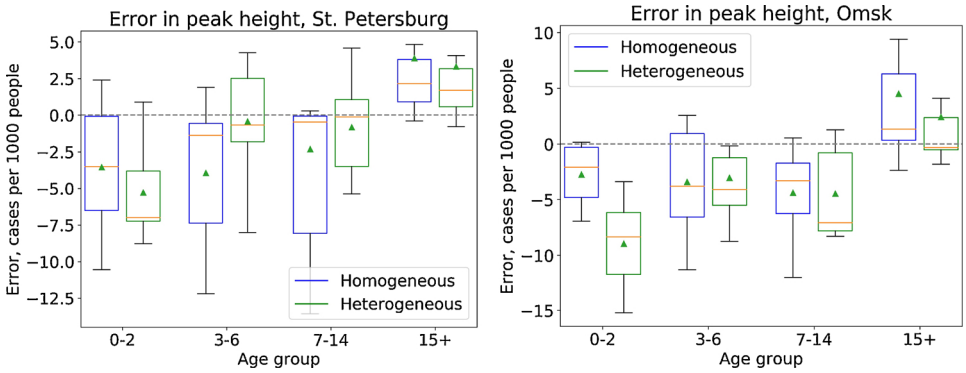

Fig. 8. Peak height assessment error, 2009–2016. Triangles depict the mean values of the samples, red lines are the medians. (For interpretation of the references to colour in this figure legend, the reader is referred to the web version of this article).

4. Discussion

In this paper, we fitted an age-dependent compartmental SEIR model to ARI incidence data in Russian cities. The results of the model calibration demonstrate the importance of distinguishing the characteristics of different age groups, such as their contact intensities and background immunity levels α_i. At the same time, the model calibration based on solely one type of data allows the existence of multiple combinations of parameters corresponding to equal values of optimization function in Eq. (4), which results in notable variation of output parameter values (see Fig. 9). We encountered the same problem while fitting the homogeneous model in application to aggregated Russian ARI incidence data (Leonenko and Ivanov, 2016). To decrease the variance of α_i and λ, the free parameters of the current model, it is crucial to employ additional sources of data. Employing external assessments on underreporting levels in different age groups might contribute to fitting accuracy of the model and help correct the parameter assessment.

It seems that the regarded ARI data do not correspond perfectly to the ARI dynamics demonstrared by an age-structured SEIR model, as it tends to underestimate incidence peaks for the age groups related to children and overestimate them in case of the group 15+. The reasons of that may lie in under-estimation of adult incidence in ARI data or in the peculiarities of the contact structure which were not captured well enough by the used contact matrix. Additional studies are required to address this discrepancy between the observed and modeled peak heights.

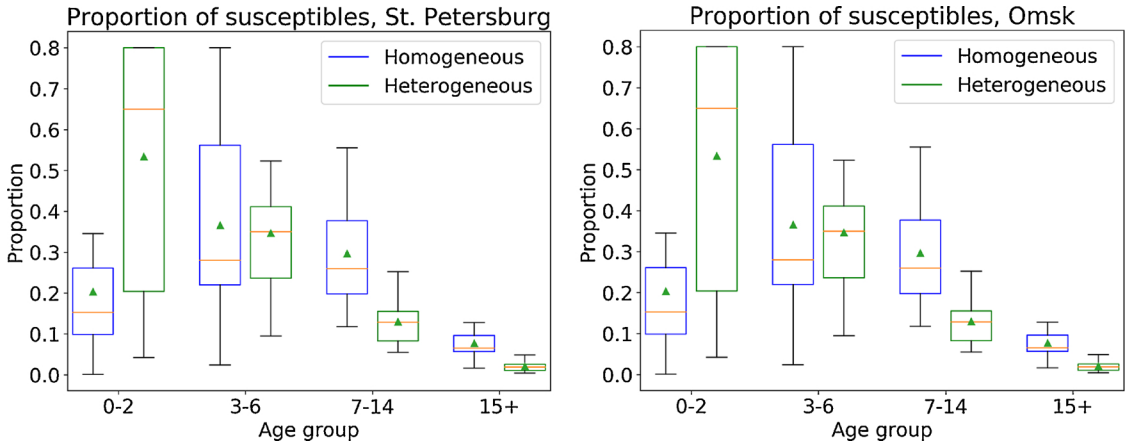

Fig. 9. Variations in proportion of susceptibles for homogeneous and heterogeneous contact patterns, 2009–2016.

Another limitation of this study is the fact that we do not distinguish the epidemics caused by A(H1N1)pdm09 and A(H3N2) strains. We plan to overcome this drawback in the future studies by using strain-specific laboratory data.

The important problem which was posed by the current research is the variability of model parameters for the age groups 0–2, 3–6, and 7–14 (i.e., the proportions of unprotected population α_i in these age groups). To help reduce the variation of α_i and thus potentially enhance the descriptive and predictive force of the model, a mechanistic submodel of background immunity dynamics might be created, taking as an input the past long-term influenza incidence data along with the topology of contact networks in particular urban settings (Bansal et al., 2010). However, this task is not easy to tackle because of lack of corresponding data and large uncertainties in parameter input. Even the detection of differences in influenza dynamics, which can be attributed to properties of urban areas, is a hard task that requires separate studies.

One of the possible ways to address the subtle properties of the influenza propagation process, which are not revealed by the aggregated models, is to employ an agent-based modeling technique regarding the epidemic outbreaks on synthetic populations constructed using explicit geographic and demographic data (Leonenko et al., 2019). This approach has already demonstrated its ability to account for the topology of human interaction networks in describing the dynamics of various diseases (Kumar et al., 2015; Geard et al., 2015) and thus may be fruitful in application to Russian flu incidence and demographic data. Such an approach could be also used to assess the disease incidence in Russian rural areas, which by now are mostly not covered by the surveillance centers.

Declaration of Competing Interest

The authors declare that they have no known competing financial interests or personal relationships that could have appeared to influence the work reported in this paper.

Acknowledgements

The work was supported by Russian Foundation for Basic Research [grant number 18-37-00428]. The authors are thankful to two anonymous reviewers whose valuable comments helped to increase the quality of the manuscript.

Appendix A. Contact matrix calculation

The aim of the procedures described below was to find a contact matrix for the age groups used in Russian ARI incidence reports, i.e. 0–2, 3–6, 7–14, and 15+. The calculations were based on a contact matrix with daily number of contacts between groups of ages 0–4, 5–9, 10–15, …, 55+ for Tomsk, Russia (Ajelli and Litvinova, 2017).

Let $C(a_{k,l}, a_{p,q})$ be the daily number of contacts with individuals of ages $a_y \in [a_p, a_q]$ that was reported by individuals of ages $a_x \in [a_k, a_l]$. Due to absense of contact data for separate ages, we assume that for any given age within a regarded age group the number of contacts is the same, i.e. for any $a_x \in [a_k, a_l]$

$$C(a_x, a_{p,q}) = C(a_{k,l}, a_{p,q}) \tag{a1}$$

Based on this assumption and the demographic data on the absolute number of individuals in different age groups, we can calculate the overall number of contacts in the population, initially between the age groups, $Q(a_{k,l}, a_{p,q})$, and then between the separate ages, $Q(a_x, a_y)$. This number of contacts is later summed for the new age groups and recalculated back to the average number of contacts per person in the new age groups.

The matrix calculation algorithm has the following structure.

- Calculate the overall number of contacts in the population between the age groups according to the formula $Q(a_{k,l}, a_{p,q}) = C(a_{k,l}, a_{p,q}) \cdot \mathrm{S}(a_{k,l})$, where $\mathrm{S}(a_{k,l})$ is the absolute number of individuals in an age group $a_{k,l}$.
- Based on (a1), calculate the overall number of contacts in the population between the ages $a_x \in [a_k, a_l]$, $a_y \in [a_p, a_q]$, according to the formula $Q(a_x, a_y) = Q(a_{k,l}, a_{p,q}) \cdot \frac{\mathrm{S}(a_x)\mathrm{S}(a_y)}{\mathrm{S}(a_{k,l})\mathrm{S}(a_{p,q})}$, where $\mathrm{S}(a_x)$ is the absolute number of individuals of age a_x.
- Calculate the overall number of contacts between the new age groups: $Q(a_{m,n}, a_{u,v}) = \sum_{x=m}^{n} \sum_{y=u}^{v} Q(a_x, a_y)$.
- Find the contact matrix for the new age groups by calculating the average number of contacts between them: $C(a_{m,\mathrm{n}}, a_{u,v}) = \frac{Q(a_{m,n}, a_{u,v})}{S(a_{m,n})}$.

Ideally, separate contact matrices should be calculated for every city under consideration, however, due to absence of detailed demographic data we used the same matrix for both Saint Petersburg and Omsk, with $\mathrm{S}(a_x)$ and $\mathrm{S}(a_{k,l})$ derived from 2017 data of Office of the Federal State Statistics Service of St. Petersburg and Leningrad region (Petrostat) (Petrostat, 2017). In the future, we plan to use contact matrices for a number of Russian cities assessed directly from the population-based surveys, which are under preparation by the research group of Ajelli et al.

Appendix B. ARI baseline assessment

Fig. B1

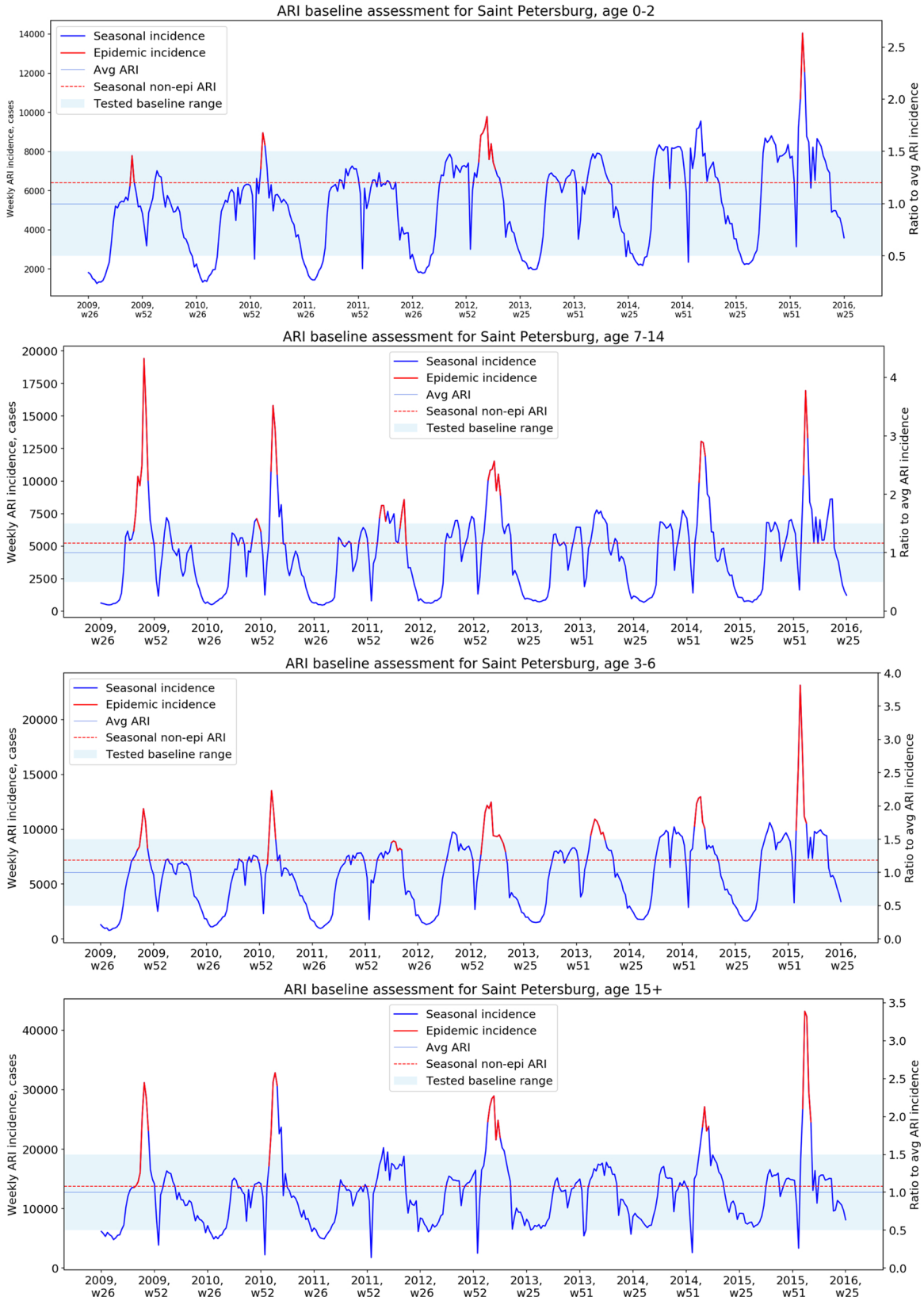

Fig. B1. ARI baseline assessment.

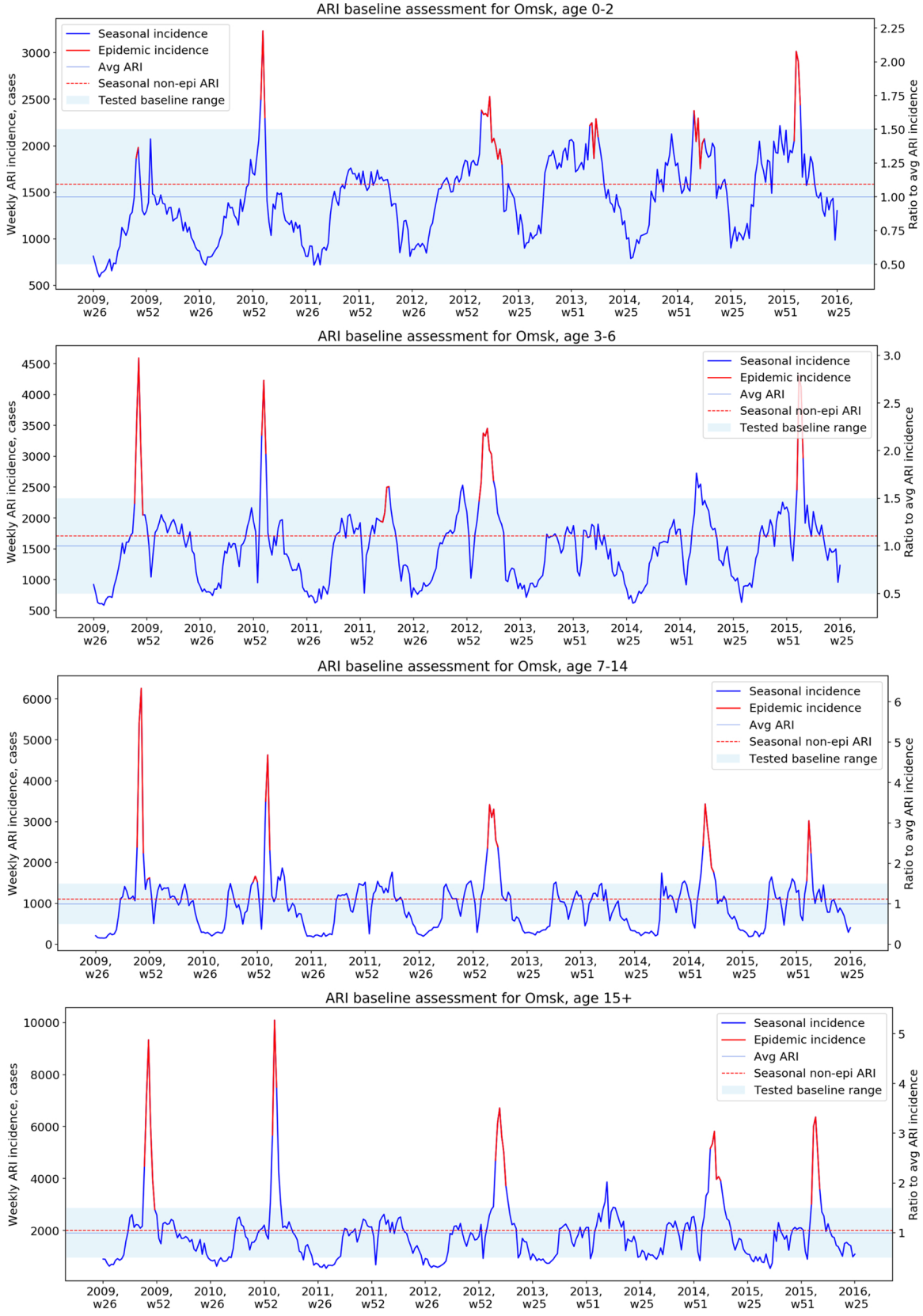

Fig. B1. (*continued*)

Appendix C. Model calibration results for the non-epidemic baseline

Fig. C1

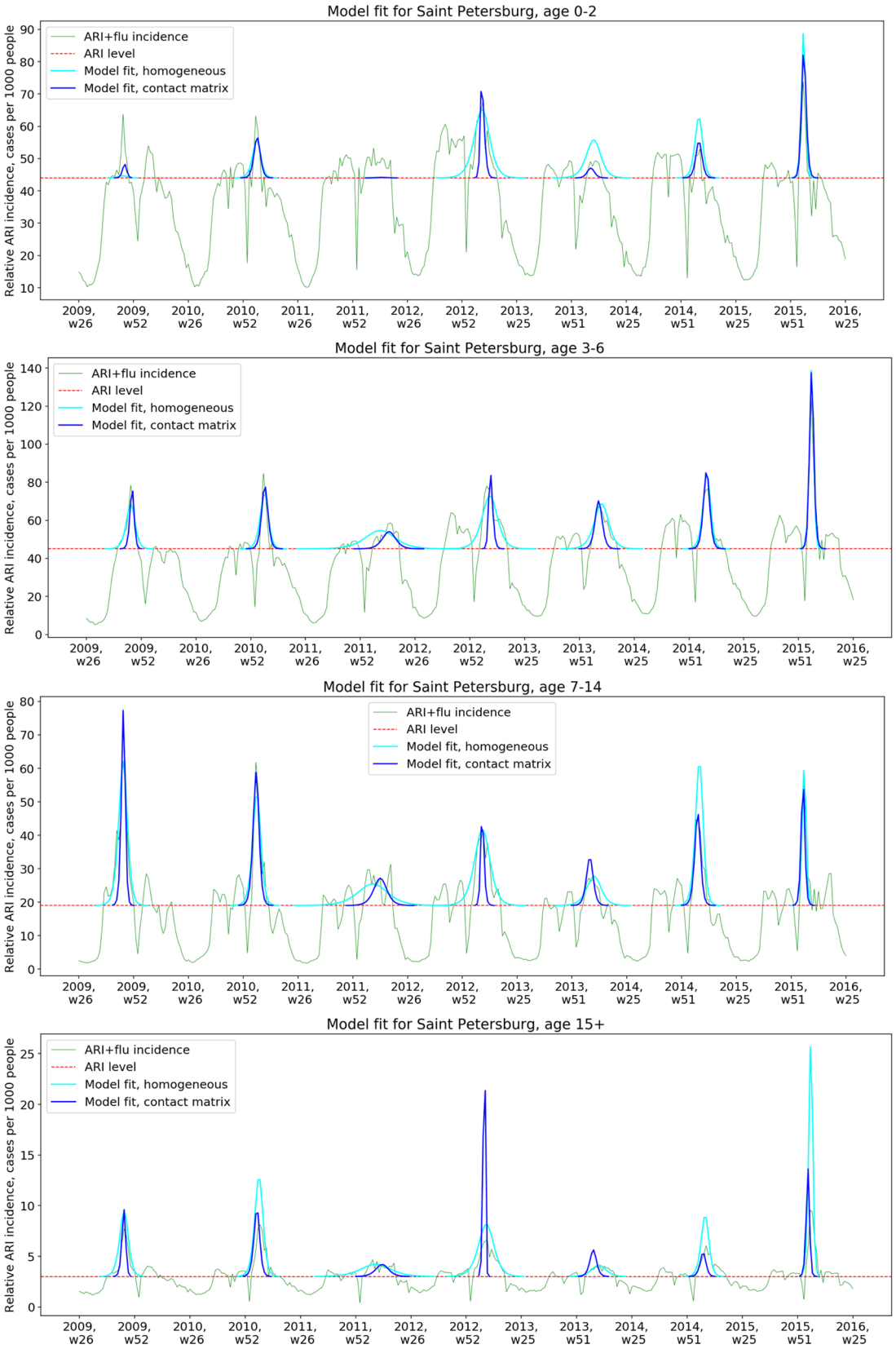

Fig. C1. Model fit for different cities and age groups.

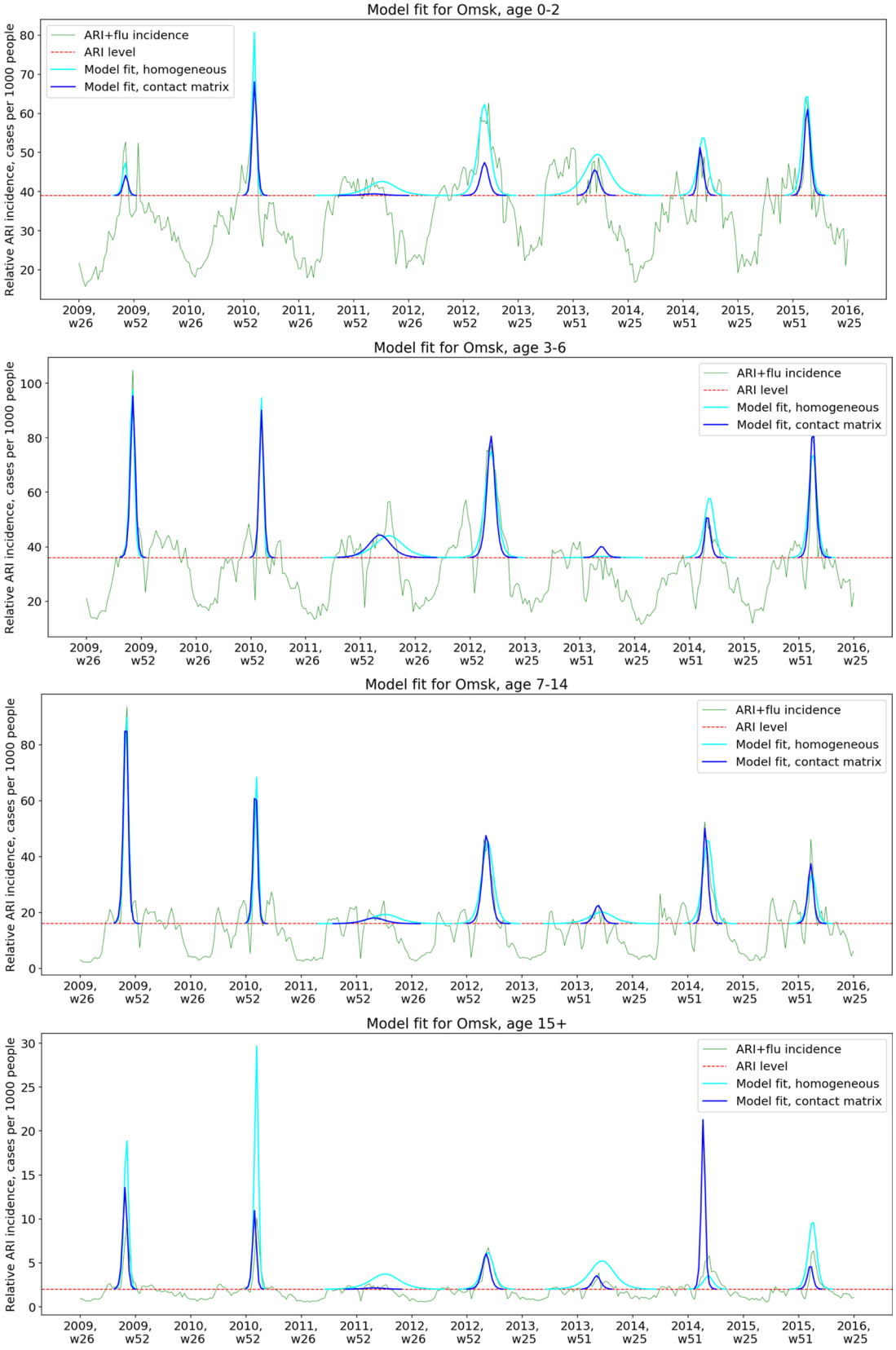

Fig. C1. (*continued*)

Appendix D. Under-reporting estimation

The recurring peak height overestimation for the age group 15+ demonstrated by the model (Section 2, Fig. 8) brought us to the idea that the cause is the underreporting of ARI cases among the adults. Relying on this assumption, we assessed the prospected real incidence for adults by excluding the ARI data for 15+ from the optimization criterion (3). The error distribution for the ARI incidence peak in the remaining three age groups is shown in Fig. D1 , left. The adult underreporting assessed with this naïve approach is demonstrated in Fig. D1, right. The corresponding confidence intervals are very wide, so it seems necessary to increase the number of calibrated outbreaks for the regarded cities to make more plausible assessments of under-reporting.

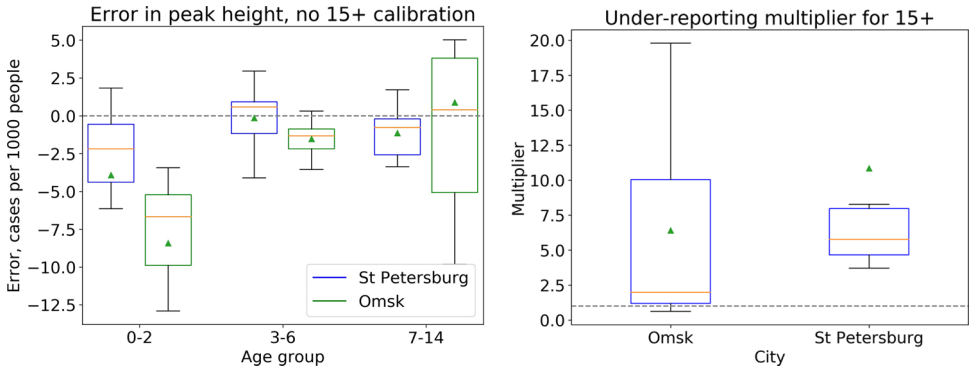

Fig. D1. Assessed adult ARI incidence underreporting in Saint Petersburg and Omsk.

Appendix E. Influence of initial parameter range on calibrated parameter values

Fig. E1

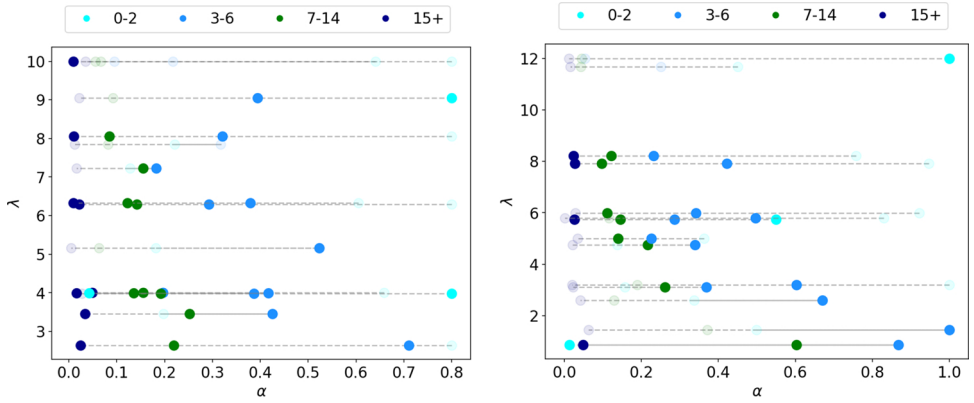

Fig. E1. Distribution of values of α_i and λ, for a non-epidemic ARI baseline and enhanced calibration algorithm. Left: standard parameter range, right: extended parameter range. Transparent points correspond to fitted curves with $R^2 < 0$. It is demonstrated that most of the parameter values (especially those corresponding to the satisfactorily fitted curves) tend to be concentrated closer to lower-left corner of the graph (lower bound of the initial intervals) and generally do not grow higher when the upper bound is extended.

References

WHO, 2014. Influenza (seasonal). Fact Sheet No. 211, March. [online]. http://www.who.int/mediacentre/factsheets/fs211/en/.

CDC, 2019. People With Heart Disease and Those Who Have Had a Stroke Are at High Risk of Developing Complications From Influenza (the Flu), [online]. http://www.cdc.gov/flu/heartdisease/.

He, D., Dushoff, J., Eftimie, R., Earn, D.J., 2013. Patterns of spread of influenza A in Canada. Proc. R. Soc. Lond. B Biol. Sci. 280 (1770), 20131174.

Shaman, J., Pitzer, V.E., Viboud, C., Grenfell, B.T., Lipsitch, M., 2010. Absolute humidity and the seasonal onset of influenza in the continental United States. PLoS Biol. 8 (2), e1000316.

Yaari, R., Katriel, G., Huppert, A., Axelsen, J., Stone, L., 2013. Modelling seasonal influenza: the role of weather and punctuated antigenic drift. J. R. Soc. Interface 10 (84), 20130298.

Truscott, J., Fraser, C., Cauchemez, S., Meeyai, A., Hinsley, W., Donnelly, C.A., Ghani, A., Ferguson, N., 2011. Essential epidemiological mechanisms underpinning the transmission dynamics of seasonal influenza. J. R. Soc. Interface rsif20110309.

Konshina, O., Sominina, A., Smorodintseva, E., Stolyarov, K., Nikonorov, I., 2017. Population immunity to influenza virus A(H1N1)pdm09, A(H3N2) and B in the adult population of the Russian federation long-term research results. Russ. J. Infect. Immun. 7 (1), 27–33. https://doi.org/10.15789/2220-7619-2017-1-27-33. in Russian.

Broniatowski, D.A., Paul, M.J., Dredze, M., 2013. National and local influenza surveillance through Twitter: an analysis of the 2012–2013 influenza epidemic. PLoS One 8

(12), e83672.
Colizza, V., Barrat, A., Barthelemy, M., Valleron, A.-J., Vespignani, A., 2007. Modeling the worldwide spread of pandemic influenza: baseline case and containment interventions. PLoS Med. 4 (1), e13.
Cauchemez, S., Valleron, A.-J., Boelle, P.-Y., Flahault, A., Ferguson, N.M., 2008. Estimating the impact of school closure on influenza transmission from sentinel data. Nature 452 (7188), 750.
Kumar, S., Piper, K., Galloway, D.D., Hadler, J.L., Grefenstette, J.J., 2015. Is population structure sufficient to generate area-level inequalities in influenza rates? An examination using agent-based models. BMC Public Health 15 (1), 947.
Nichol, K.L., Tummers, K., Hoyer-Leitzel, A., Marsh, J., Moynihan, M., McKelvey, S., 2010. Modeling seasonal influenza outbreak in a closed college campus: impact of pre-season vaccination, in-season vaccination and holidays/breaks. PLoS One 5 (3), e9548.
Smieszek, T., Balmer, M., Hattendorf, J., Axhausen, K.W., Zinsstag, J., Scholz, R.W., 2011. Reconstructing the 2003/2004 H3N2 influenza epidemic in switzerland with a spatially explicit, individual-based model. BMC Infect. Dis. 11 (1), 115.
Baguelin, M., Flasche, S., Camacho, A., Demiris, N., Miller, E., Edmunds, W.J., 2013. Assessing optimal target populations for influenza vaccination programmes: an evidence synthesis and modelling study. PLoS Med. 10 (10), e1001527.
Goeyvaerts, N., Willem, L., Van Kerckhove, K., Vandendijck, Y., Hanquet, G., Beutels, P., Hens, N., 2015. Estimating dynamic transmission model parameters for seasonal influenza by fitting to age and season-specific influenza-like illness incidence. Epidemics 13, 1–9.
Yamana, T.K., Kandula, S., Shaman, J., 2017. Individual versus superensemble forecasts of seasonal influenza outbreaks in the United States. PLoS Comput. Biol. 13 (11), e1005801.
Ivannikov, Y.G., Ismagulov, A.T., 1983. Epidemiologiya Grippa (The Epidemiology of Influenza), Almaty, Kazakhstan. In Russian.
Cliff, A.D., Haggett, P., Ord, J.K., 1986. Spatial Aspects of Influenza Epidemics. Routledge.
Research Institute of Influenza website, 2019. Research Institute of Influenza website [online]. http://influenza.spb.ru/en/.
WHO, 2019a. Influenza Surveillance Country, Territory and Area Profiles 2017, [online]. http://www.euro.who.int/_data/assets/pdf_file/0007/356119/InfluenzaSurveillanceProfiles_2017_en.pdf.
Baroyan, O., Basilevsky, U., Ermakov, V., Frank, K., Rvachev, L., Shashkov, V., 1970. Computer modelling of influenza epidemics for large-scale systems of cities and territories. Proc. WHO Symposium on Quantitative Epidemiology.
Leonenko, V.N., Ivanov, S.V., 2018. Influenza peaks prediction in Russian cities: comparing the accuracy of two SEIR models. Math. Biosci. Eng. 15 (1), 209–232. https://doi.org/10.3934/mbe.2018009.
Wallinga, J., Teunis, P., Kretzschmar, M., 2006. Using data on social contacts to estimate age-specific transmission parameters for respiratory-spread infectious agents. Am. J. Epidemiol. 164 (10), 936–944.
Ajelli, M., Litvinova, M., 2017. Estimating contact patterns relevant to the spread of infectious diseases in Russia. J. Theor. Biol. 419, 1–7.
Mossong, J., Hens, N., Jit, M., Beutels, P., Auranen, K., Mikolajczyk, R., Massari, M., Salmaso, S., Tomba, G.S., Wallinga, J., et al., 2008. Social contacts and mixing patterns relevant to the spread of infectious diseases. PLoS Med. 5 (3), e74.
Marinich, I.G., Karpova, L.S., Kondratyev, V., 2005. Methodological Recommendations for the Operational Analysis and Forecasting of the Epidemiological Situation on Influenza and Acute Respiratory Infections (ARI), Moscow. in Russian.
Leonenko, V.N., Ivanov, S.V., Novoselova, Y.K., 2016a. A computational approach to investigate patterns of acute respiratory illness dynamics in the regions with distinct seasonal climate transitions. Procedia Comput. Sci. 80, 2402–2412.
Romanyukha, A., Sannikova, T., Drynov, I., 2011. The origin of acute respiratory epidemics. Her. Russ. Acad. Sci. 81 (1), 31–34.
Kirkpatrick, S., Gelatt, C.D., Vecchi, M.P., 1983. Optimization by simulated annealing. Science 220 (4598), 671–680. https://doi.org/10.1126/science.220.4598.671.
Seleznev, N.E., Leonenko, V.N., 2017. Boosting Performance of Influenza Outbreak Prediction Framework, in: Digital Transformation and Global Society. Springer International Publishing, pp. 374–384. https://doi.org/10.1007/978-3-319-69784.
Liu, D.C., Nocedal, J., 1989. On the limited memory BFGS method for large scale optimization. Math. Program. 45 (1-3), 503–528.
Rahmandad, H., Sterman, J., 2008. Heterogeneity and network structure in the dynamics of diffusion: comparing agent-based and differential equation models. Manage. Sci. 54 (5), 998–1014.
Leonenko, V.N., Novoselova, Y.K., Ong, K.M., 2016b. Influenza outbreaks forecasting in Russian cities: Is Baroyan-Rvachev approach still applicable? Procedia Comput. Sci. 101, 282–291.
Leonenko, V.N., Ivanov, S.V., 2016. Fitting the SEIR model of seasonal influenza outbreak to the incidence data for Russian cities. Russ. J. Numer. Anal. Math. Model. 31 (5), 267–279.
Geard, N., Glass, K., McCaw, J.M., McBryde, E.S., Korb, K.B., Keeling, M.J., McVernon, J., 2015. The effects of demographic change on disease transmission and vaccine impact in a household structured population. Epidemics 13, 56–64. https://doi.org/10.1016/j.epidem.2015.08.002.
Flu Near You, 2019. Flu Near You [online]. https://flunearyou.org.
Karpova, L.S., et al., 2014. Comparison of Pandemic Influenza A(H1N1)pdm09 in Russia 2009–2010 with Subsequent Epidemics involving influenza (2011–2014). Epidemiologiya i Vaktsinoprofilaktika 6 (79), 8–16 in Russian.
Bansal, S., Pourbohloul, B., Hupert, N., Grenfell, B., Meyers, L.A., 2010. The shifting demographic landscape of pandemic influenza. PLoS One 5 (2), e9360. https://doi.org/10.1371/journal.pone.0009360.
Leonenko, V., Lobachev, A., Bobashev, G., 2019. Spatial modeling of influenza outbreaks in Saint Petersburg using synthetic populations. International Conference on Computational Science. Springer, Cham, pp. 492–505 Jun 12.
Age and sex composition of the population of St. Petersburg as at January 1st of 2017 ("Vozrastno-polovoy sostav naseleniya Sankt-Peterburga na 1 yanvarya 2017"). Statistical Bulletin, Saint Petersburg, Petrostat (In Russian).
WHO, 2019b. Surveillance Case Definitions for ILI and SARI, [online]. http://www.who.int/influenza/surveillance_monitoring/ili_sari_surveillance_case_definition/en/.